

---

# Patient-Specific Dosimetry in Predicting Renal Toxicity with $^{90}\text{Y}$ -DOTATOC: Relevance of Kidney Volume and Dose Rate in Finding a Dose–Effect Relationship

Raffaella Barone, MD<sup>1</sup>; Françoise Borson-Chazot, MD, PhD<sup>1</sup>; Roelf Valkema, MD, PhD<sup>2</sup>; Stéphan Walrand, PhD<sup>1</sup>; Franck Chauvin, MD, PhD<sup>3</sup>; Lida Gogou, MD<sup>1</sup>; Larry K. Kvols, MD<sup>4</sup>; Eric P. Krenning, MD, PhD<sup>2</sup>; François Jamar, MD, PhD<sup>1</sup>; and Stanislas Pauwels, MD, PhD<sup>1</sup>

<sup>1</sup>Centre of Nuclear Medicine and Laboratory of Positron Emission Tomography; Université Catholique de Louvain, Brussels and Louvain-la-Neuve, Belgium; <sup>2</sup>Department of Nuclear Medicine, Erasmus Medical Center, Rotterdam, The Netherlands; <sup>3</sup>Department of Biostatistics, Centre Léon Bérard, Lyon, France; <sup>4</sup>H. Lee Moffitt Cancer Center and Research Institute, University of South Florida, Tampa, Florida

Nephrotoxicity is the major limiting factor during therapy with the radiolabeled somatostatin analog  $^{90}\text{Y}$ -1,4,7,10-tetraazacyclododecane-*N,N',N'',N'''*-tetraacetic acid (DOTA)-D-Phe<sup>1</sup>-Tyr<sup>3</sup>-octreotide (DOTATOC). Pretherapeutic assessment of kidney absorbed dose could help to minimize the risk of renal toxicity. The aim of this study was to evaluate the contribution of patient-specific adjustments to the standard dosimetric models, such as the renal volume and dose rate, for estimating renal absorbed dose during therapy with  $^{90}\text{Y}$ -DOTATOC. In particular, we investigated the correlation between dose estimates and effect on renal function after therapy. **Methods:** Eighteen patients with neuroendocrine tumors (9 men and 9 women; median age, 59 y) underwent treatment with  $^{90}\text{Y}$ -DOTATOC (8.1–22.9 GBq) after pretherapeutic biodistribution study with  $^{86}\text{Y}$ -DOTATOC. Kidney uptake and residence times were measured and the absorbed dose (KAD) was computed using either the MIRDOSE3.1 software assuming a standard kidney volume ( $\text{KAD}_{\text{StdVol}}$ ) or the MIRD Pamphlet 19 values and the actual kidney cortex volume determined by pretherapeutic CT ( $\text{KAD}_{\text{CTVol}}$ ). For each patient, the biologic effective dose (BED) was calculated according to the linear quadratic model to take into account the effect of dose rate and fractionation. Renal function was evaluated every 6 mo by serum creatinine and creatinine clearance (CLR) during a median follow-up of 35.5 mo (range, 18–65 mo). The individual rate of decline of renal function was expressed as CLR loss per year. **Results:**  $\text{KAD}_{\text{CTVol}}$  ranged between 19.4 and 39.6 Gy (mean,  $28.9 \pm 5.34$  Gy). BED, obtained from  $\text{KAD}_{\text{CTVol}}$ , ranged between 27.7 and 59.3 Gy (mean,  $40.4 \pm 10.6$  Gy). The CLR loss per year ranged from 0% to 56.4%. In 12 of 18 patients, CLR loss per year was <20%. No correlation was observed between CLR loss per year and the  $\text{KAD}_{\text{StdVol}}$  or the  $\text{KAD}_{\text{CTVol}}$ . In contrast, BED strongly correlated with CLR loss per year ( $r = 0.93$ ;  $P < 0.0001$ ). All 5 patients with

CLR loss per year >20% received a BED >45 Gy. Patients who were treated with low fractionation were those with the highest rate of renal function impairment. **Conclusion:** Radiation nephrotoxicity after  $^{90}\text{Y}$ -DOTATOC therapy is dose dependent. Individual renal volume, dose rate, and fractionation play important roles in an accurate dosimetry estimation that enables prediction of risk of renal function impairment.

**Key Words:** kidney dosimetry;  $^{90}\text{Y}$ -DOTA-Tyr<sup>3</sup>-octreotide; radionuclide therapy; radiation nephropathy

**J Nucl Med 2005; 46:99S–106S**

**P**eptide receptor radionuclide therapy (PRRT) using radiolabeled somatostatin analogs appears to be promising for the treatment of somatostatin receptor–positive neuroendocrine tumors (1–3). In patients who are untreatable by other conventional methods, favorable clinical responses were obtained with 1,4,7,10-tetraazacyclododecane-*N,N',N'',N'''*-tetraacetic acid (DOTA)-D-Phe<sup>1</sup>-Tyr<sup>3</sup>-octreotide (DOTA-TOC) labeled with  $^{90}\text{Y}$ , a high-energy  $\beta$ -emitter (2–7). Because a clear dose–response relationship was shown between reduction in tumor volume and tumor radiation dose, the challenge is to deliver the highest activity to the tumor while sparing normal tissues (8,9). Recent biodistribution studies and clinical trials showed that the kidney is a major critical organ for PRRT with  $^{90}\text{Y}$ -DOTATOC (10–17). The radiolabeled peptide is rapidly cleared from the circulation by the kidneys and, after filtration by the glomeruli, is reabsorbed and retained into the proximal tubular cells. Renal toxicity after treatment was reported in 6 cases (13–17). In the largest published series, Otte et al. (13) reported 4 cases with renal damage among 29 patients treated. Radiation-induced thrombotic microangiopathy was identified on kidney biopsy samples.

---

Received Sep. 8, 2004; revision accepted Nov. 2, 2004.  
For correspondence or reprints contact: Stanislas Pauwels, MD, PhD, Centre de Médecine Nucléaire, Université Catholique de Louvain, UCL 54.30, Avenue Hippocrate, 54, B-1200 Brussels, Belgium.  
E-mail: stanislas.pauwels@mnucl.ucl.ac.be

Several factors could be involved in renal damage, among which absorbed dose to kidneys is likely to play a key role. With fractionated external beam radiotherapy, the dose resulting in a 5% probability of developing radiation nephropathy within 5 y was found to be 23 Gy (18). However, in PRRT, where the dose rate is much lower and the radiation delivered to organs is inhomogeneous, the critical dose may be higher and has not yet been determined (19).

Because of the large variability in individual renal uptake of <sup>90</sup>Y-DOTATOC, some patients could potentially receive critical kidney doses, particularly if high activities are administered to deliver the most effective tumor doses (10). Therefore, in a recent therapeutic trial with <sup>90</sup>Y-DOTATOC, we implemented a patient-specific therapeutic regimen approach. Individual activities administered were based on a pretherapeutic absorbed dose estimate using <sup>86</sup>Y-DOTA-TOC for quantitative kidney imaging and the MIRDOSE3.1 model (20). On the basis of these individual absorbed dose estimations, the administered activities were calculated to deliver a cumulative absorbed dose to the kidneys close to 27 Gy. In spite of the fact that the treatment was planned to deliver a similar absorbed dose to each patient, a wide interpatient difference in kidney side effects was observed during follow-up. These findings suggest that either the absorbed dose alone would not predict response or that conventional dosimetry analyses, based on stylized formalisms, are oversimplified and thus lack the accuracy needed to be valid predictors of toxicity. This retrospective study was undertaken in a subset of those patients to evaluate

whether implementation of a more refined absorbed dose estimation method, including adjustments for the actual volume of the irradiated organ and the dose rate effect, would result in greater clinical relevance.

## MATERIALS AND METHODS

### Study Design and Patients

The study group represented a subset of patients with neuroendocrine tumors, enrolled in a phase 1 multicenter study intended to establish the 1-cycle and multiple-cycle maximum tolerated doses of <sup>90</sup>Y-DOTATOC (Novartis Pharma AG) in patients with metastatic, somatostatin-receptor positive tumors (21). The study was approved by the Ethics Committee of the University of Louvain Medical School, and all patients gave written informed consent.

This retrospective study was restricted to patients with gastroenteropancreatic tumors in whom pretherapeutic abdominal CT allowed accurate determination of kidney volume and who were followed up for at least 18 mo. Clinical characteristics are summarized in Table 1. The study included 9 women and 9 men (ages, 41–75 y; mean, 57.2 ± 8.9 y) with histologically confirmed tumor(s) and positive <sup>111</sup>In-pentetreotide (OctreoScan111; Tyco Healthcare) imaging. Disease extent was assessed by CT. Three patients had undergone previous chemotherapy more than 6 mo before PRRT, 4 were diabetic, and 4 were hypertensive. Each patient underwent pretherapeutic biodistribution and pharmacokinetic studies with <sup>86</sup>Y-DOTATOC PET to measure individual kidney uptake and estimate <sup>90</sup>Y-labeled analog renal absorbed doses during therapy (10). This study allowed individualized treatment of patients with cumulative activities that would not exceed the safety threshold of 27 Gy to kidney. All 18 patients were

**TABLE 1**  
Patients and Treatment Characteristics

Patient	Diagnosis	Age (y)	Sex	BSA (m <sup>2</sup> )	Injected activities					Follow-up (mo)
					Cycle 1 (GBq)	Cycle 2 (GBq)	Cycle 3 (GBq)	Cycle 4 (GBq)	Cycle 5 (GBq)	
1	Carcinoid	64	F	1.58	2.9	2.9	2.9	2.9		64.1
2	Islet cell F	75	F	1.73	2.9	2.9	2.9	2.9		64.8
3	Islet cell NF	63	F	1.50	4.0	3.9	3.9	3.7		62.2
4	Carcinoid	47	F	1.50	3.3	3.3	3.3	3.3		18.0*
5	Carcinoid	64	M	1.94	9.0	2.5				38.2
6	Carcinoid	57	F	1.95	10.5	5.3				19.6
7	Carcinoid	42	M	1.55	10.0	10.0				34.1
8	Islet cell NF	63	M	1.68	11.6	3.0				26.8
9	Carcinoid	60	M	1.82	13.7	4.7	4.5			28.0
10	Carcinoid	62	M	1.74	11.0					18.7
11	Islet cell NF	63	M	1.88	3.4	3.4	3.4	3.4	3.3	61.4
12	Islet cell F	43	F	1.51	3.8	3.8	3.8	3.8		51.3
13	Unclassified	55	M	2.06	9.3	5.9				45.3
14	Islet cell NF	63	M	1.78	14.4	4.6				23.0
15	Islet cell F	44	F	1.75	2.6	2.5	2.5	2.5		18.0
16	Carcinoid	58	M	1.81	1.7	1.5	1.7	1.7	1.7	24.1*
17	Islet cell F	55	F	1.75	2.1	2.1	2.1	2.1		65.4
18	Carcinoid	52	F	1.64	7.5	3.7				36.0

\*Patient died from tumor progression during follow-up.

BSA = body surface area; carcinoid = carcinoid tumor; islet cell F = functioning islet cell carcinoma; islet cell NF = nonfunctioning islet cell carcinoma.

subsequently treated, under amino acid infusion, with  $^{90}\text{Y}$ -DOTATOC (21). The median follow-up was 35.5 mo (range, 18.0–65.4 mo).

### Assessment of Renal Function

During follow-up, kidney function was assessed every 6 mo by serum creatinine and by creatinine clearance (CLR). Measured CLR was determined based on 2 24-h urine collections and serum creatinine assessment. This method is prone to sampling errors and may vary by 10%–20% from day to day. During follow-up, changes in CLR were assessed by estimated CLR using the Cockcroft–Gault formula:

$$\text{CLR} = (140 - \text{age} [\text{y}]) \times (\text{weight} [\text{kg}]) \times 1.23/(\text{s-creat}[\mu\text{mol/L}]), \quad \text{Eq. 1}$$

for men, multiplied by 0.85 for women (22). At baseline, we calculated the ratio between true CLR and the estimated CLR for each patient. All subsequent estimated CLR values were multiplied by this factor to yield CLR.

The kidney is an organ with a slow cellular turnover, and radiation-induced functional damage appears with a substantial delay. It is therefore important to observe renal function over a long period of time to assess the long-term risk of clinically relevant loss of function. Because the follow-up duration varied for each patient in this study, we evaluated individual rates of decline of renal function, expressed as CLR loss per year. To determine the percentage change in CLR per year, a monoexponential curve was fitted through the CLR data of each patient, from the start of treatment onward (23).

### Kidney Volume Determination from CT Scan

Kidney volume was retrospectively measured (by an individual unaware of patient characteristics) on pretherapeutic CT scan by drawing regions of interest (ROIs) on consecutive transverse slices including the whole kidneys and the intrarenal part of the collecting system. Intra- and interobserver coefficients of variation were 3.4% and 3.8%, respectively. In this study, the same observer performed all measurements. In 12 patients, kidney volume was also measured on CT scans obtained at the end of treatment to evaluate the effect of treatment on kidney volume. We assumed that the renal cortex accounted for 70% of total kidney volume (24).

### Estimation of Kidney Absorbed Dose Using $^{86}\text{Y}$ -DOTATOC PET Imaging

*Tracers and Reagents.* DOTATOC (Novartis Pharma AG) was available as a lyophilized kit.  $^{86}\text{Y}$  was produced by irradiation of enriched  $^{86}\text{SrCO}_3$  (Oak Ridge National Laboratory [ORNL]) after an  $^{86}\text{Sr}(p,n)^{86}\text{Y}$  reaction (25). Radiolabeling was performed as previously described (10). The final injected activity was  $286 \pm 119$  MBq. The study was performed with co-infusion of mixed amino acids (10). A commercially available amino acid solution was used: 1,500 mL Proteinsteril Hepa 8% (Fresenius) containing 10.72 g L-arginine and 6.88 g L-lysine per liter together with other essential and nonessential amino acids, was brought to 1,800 mL by addition of 300 mL lactated Ringer's solution (Hartmann; Travenol Laboratories). The total L-arginine + L-lysine amount was 26.4 g. This solution was infused over 4 h, starting 30 min before  $^{86}\text{Y}$ -DOTATOC. The same renal protection regimen was applied for  $^{90}\text{Y}$ -DOTATOC treatment.

*$^{86}\text{Y}$ -DOTATOC Biodistribution.*  $^{86}\text{Y}$ -DOTATOC PET was performed at 3.5, 24, and 48 h after injection. A transmission scan using rotating-rod  $^{68}\text{Ge}$  sources was acquired before injection. The camera used was an ECAT EXACT HR tomograph (Siemens-CTI) (26), operated in two-dimensional mode (i.e., with septa extended). Ten overlapping 5-min bed positions (15 cm, 2.5 cm overlap) were acquired at 3.5 h. At 24 and 48 h only, 3–6 positions were acquired on the main field of interest for a total duration of 60 min. The scans were reconstructed by iterative processing (OSEM) in a  $128 \times 128$  matrix (pixel size, 4.3 mm), with decay and attenuation corrections as well as correction for spurious photon contamination arising from the high-energy  $\gamma$ -emissions of  $^{86}\text{Y}$  (27,28). A noise filter of 9-mm spatial resolution was applied.

*Data Processing.* For quantification of kidney radioactivity uptake, ROIs were drawn plane by plane on all transverse consecutive PET slices, and the activity was expressed as a percentage of injected activity. In patient 14, the upper pole of the left kidney could not be accurately delineated because of overlying tumor activity. The initial quantification was performed assuming that the total uptake of the left kidney was equal to the uptake measured in its lower part, corrected for the total volume of the right kidney, and that both kidneys had similar volumes. When we reanalyzed data for this report, we found in patient 14 a larger difference between the volumes of the 2 kidneys, and, therefore, we corrected the quantitative uptake data, taking into account the actual CT volume of the left kidney.

Residence time in kidneys was calculated from uptake measurements. Linear fitting was used between 4 and 24 h and extrapolated to time 0. Washout curves were fitted to a monoexponential function between 24 and 48 h and applied onward. The effective half-life of  $^{90}\text{Y}$ -DOTATOC ( $T_{1/2}^{\text{eff}}$ ) was also estimated. Residence time values were input into the MIRDSE3.1 program to calculate dosimetry estimates for  $^{90}\text{Y}$ -DOTATOC in a reference man or woman. Kidney cortex radiation doses were also computed by rescaling the individual dose obtained from MIRD Pamphlet 19 using the ratio between standard kidney volume (288 mL) and the actual renal cortex volume, assuming that cortex volume accounted for 70% of the total kidney CT estimate (24). S factors given by MIRD Pamphlet 19 account for energy loss in the kidney medulla from the cortex, thereby providing a more accurate calculation of the dose to the cortex.

### Calculation of Biologic Effective Dose Using the Linear–Quadratic Model

The linear–quadratic (LQ) model describes the surviving fraction (S) of target cells after a radiation dose (D):

$$S = e^{-\alpha D - \beta D^2}, \quad \text{Eq. 2}$$

where the linear component  $\alpha D$  describes the double-strand breaks induced by a single ionizing event, and the quadratic component  $\beta D^2$  describes the same effect induced by 2 separate ionizing events.

This model applied to a therapeutic dose delivered over a period of time and fractionated in multiple cycles gives an estimation of the biologic effective dose (BED) (19):

$$\text{BED} = \sum_i D_i + \frac{\beta}{\alpha} \frac{T_{1/2}^{\text{rep}}}{T_{1/2}^{\text{rep}} + T_{1/2}^{\text{eff}}} \sum_i D_i^2, \quad \text{Eq. 3}$$

where  $D_i$  is the dose delivered for cycle  $i$ ;  $T_{1/2}^{\text{eff}}$  is the effective half-life of  $^{90}\text{Y}$ -DOTATOC based on  $^{86}\text{Y}$ -DOTATOC individual biodistribution data; and  $T_{1/2}^{\text{rep}}$  is the repair half-time of sublethal damage.

It should be pointed out that the nonlinearity of Equation 3 requires that dose  $D_i$  be the absolute amount of energy delivered per mass unit of tissue.

We assumed that  $T_{1/2}^{rep} = 2.8$  h and  $\alpha/\beta = 2.6$  Gy, as reported in the literature (29).

### **<sup>90</sup>Y-DOTATOC Administration Protocol**

Patients were treated in the framework of a phase 1 dose-escalation study aiming to evaluate the safety of <sup>90</sup>Y-DOTATOC (21). The treatment consisted of a single or multiple cycles given at 6- to 9-wk intervals. Dose escalation proceeded in both a vertical and horizontal manner. As mentioned previously, the individual treatment regimen was planned aiming not to exceed the safety threshold of 27 Gy to kidney. Individual activities administered and the number of therapeutic cycles are listed in Table 1. The number of cycles varied from 1 to 5. The median cumulated activity administered was 14.0 GBq, ranging between 8.1 and 22.9 GBq. Total renal absorbed dose, estimated from MIRDOSE3.1, ranged from 25.6 to 38.6 Gy (median, 27.1 Gy) (Table 2). In 2 patients, renal absorbed dose exceeded 27 Gy because of an extra-cycle <sup>90</sup>Y-DOTATOC administration (patients 11 and 16). In patient 14, the estimated renal absorbed dose increased from 27.1 to 38.6 Gy according to the calculations described here.

### **Analysis**

Results are presented as mean and SD of the mean. The 2-sample paired and unpaired Student *t* tests were used for group comparisons. The statistical significance of the difference in all comparisons was based on 1-tailed 5%  $\alpha$ -error. Correlations between the percentage of change in renal function parameters and the cumulated absorbed dose were fitted by using a modified power exponential function:

$$F(D) = (1 - e^{-aD})^b, \quad \text{Eq. 4}$$

where *F* is the function to be fitted and *D* is the kidney absorbed dose or the BED.

This formula describes well the absence of alteration for low doses (parameter *b*) followed by a fast increase (parameter *a*). Correlation *r* and significance *P* were derived from this fit.

## **RESULTS**

### **Renal Function**

As shown in Table 3, renal function was normal before treatment in all patients. After treatment, for the whole group, the mean CLR loss per year was 15.3%, ranging from 0% to 56.4%. CLR loss per year was less than 10% in 12 of 18 patients and exceeded 20% in patients 2, 8, 9, 10, and 14. During follow-up, these 5 patients exhibited a sustained and progressive increase in serum creatinine (ranging from 50% to 322%) together with a decrease in estimated CLR (ranging from 36% to 78%). In patients 2 and 9, the occurrence of proteinuria, hypertension, and edema, together with anemia and a dramatic decrease in serum haptoglobin, demonstrated radiation-induced microangiopathy. The diagnosis was biopsy-proven in patient 2. Among the 5 patients who presented major CLR loss per year, patient 14 was diabetic, with preexisting hypertension and previous chemotherapy, and patients 2 and 10 were hypertensive at baseline.

Patient 1, who also had preexisting hypertension, showed an intermediate rate of CLR loss (14%/y). However, during a 5-y follow-up she exhibited a progressive deterioration of renal function, leading to 49% CLR reduction at the last control. In addition to patient 14, the 2 other patients (6 and 13) who had undergone chemotherapy did not exhibit marked renal function decline during follow-up (CLR losses per year of 2.8% and 4.4%, respectively).

### **Kidney Volume**

As shown in Table 2, there was wide variability in kidney volumes, from 231 to 503 mL. Mean kidney volume differed between males and females ( $372.8 \pm 75.5$  and  $317.2 \pm 59.1$  mL, respectively). In all except 2 patients, kidney volume was larger than the standard ORNL phantom (i.e., the volume used to compute the dose in the MIRDOSE3.1: 288.0 mL in males and 264.4 mL in females) (Fig. 1). Patients 2 and 9, who had renal volumes smaller than the standard volume, were the same patients who demonstrated radiation-induced microangiopathy. Kidney volumes were unchanged before and after therapy.

### **Estimation of Kidney Absorbed Dose**

The median kidney uptakes of <sup>86</sup>Y-DOTATOC at 4, 24, and 48 h were 1.90%, 2.01%, and 1.54%, respectively. Median residence time was 1.09 h, ranging between 0.65 and 2 h. Assuming a standard kidney volume, the median kidney absorbed dose estimated from individual PET data was 2.05 mGy/MBq, ranging between 1.18 and 3.60 mGy/MBq (Fig. 2). Taking into account the therapeutic admin-

**TABLE 2**

Individual Estimates of Absorbed Dose to Kidneys

Patient	Kidney volume* (mL)	KAD <sub>StdVol</sub> (Gy)	KAD <sub>CTVol</sub> (Gy)	BED (Gy)
1	278	26.6	31.9	38.1
2	231	27.5	39.6	54.8
3	283	27.0	31.7	40.5
4	337	27.5	27.2	33.8
5	503	27.0	19.4	27.7
6	411	26.2	21.2	30.2
7	365	26.8	26.6	36.3
8	299	27.1	32.8	56.0
9	278	27.1	35.2	56.1
10	343	27.2	28.6	50.8
11	408	30.0	26.6	31.0
12	288	25.6	29.6	35.5
13	427	26.1	22.1	31.5
14	433	38.6	32.2	59.3
15	404	28.0	23.0	28.1
16	299	29.2	35.4	41.0
17	321	26.7	27.6	33.1
18	302	27.0	29.7	42.7

\*Sum of both kidneys.

KAD<sub>StdVol</sub> = kidney absorbed dose estimated using MIRDOSE3.1; KAD<sub>CTVol</sub> = kidney absorbed dose estimated using S values from MIRD Pamphlet 19 and rescaled for kidney volume individually measured by CT. BED = biologic effective dose.



**TABLE 3**  
Evolution of Renal Function

Patient	S-creat baseline ( $\mu\text{mol/L}$ )	$\Delta\text{S-creat}$ at 18 mo (%)	$\Delta\text{S-creat}$ last control (%)	CLR baseline (mL/min)	$\Delta\text{CLR}$ at 18 mo (%)	$\Delta\text{CLR}$ last control (%)	CLR loss per year (%)
1	97	22.7	63.9	85	32.6	49.4	14
2	92	53.3	321.7	56	38.4	78.1	26
3	61	8.2	0.0	75	4.2	3.3	4.2
4	66	-33.3	-33.3	116	0	0	0
5	97	17.5	9.3	128	7.8	1.7	1.4
6	70	-10.0	-10.0	123	11.5	11.5	2.8
7	70	0	12.9	107	8.0	8.0	9.9
8	80	110.0	110.0	107	54.9	54.9	38.8
9	97	219.0	219.0	88	68.2	71.0	56.4
10	88	50.0	50.0	71	39.3	36.3	45.7
11	77	9.1	-2.6	100	7.74	1.5	2
12	65	-9.2	-10.8	85	0	0	0
13	75	1.3	-1.3	119	0	4.2	4.4
14	88	125.0	146.6	63	61	64.8	51.3
15	53	11.3	11.3	115	10.2	10.2	3.1
16	69	24.6	26.1	108	20.2	22.5	9.4
17	71	12.7	-11.3	93	20.3	5.7	0.9
18	71	9.9	-2.8	80	9.8	7.2	5.9

$\Delta\text{S-creat}$  at 18 mo = maximum percentage change in serum creatinine at 18-mo follow-up;  $\Delta\text{S-creat}$  last control = percentage changes in serum creatinine at last control of individual follow-up period;  $\Delta\text{CLR}$  at 18 mo = maximum percentage changes in CLR at 18-mo follow-up;  $\Delta\text{CLR}$  last control = percentage changes in CLR at last control of individual follow-up period; CLR loss per year = annual rate of CLR loss determined using exponential fit of CLR values. CLR was estimated by Cockcroft–Gault formula and corrected by each individual correction factor calculated to compensate for ratio between true CLR and CLR estimated by Cockcroft–Gault formula at baseline.

istered activities, the individual kidney absorbed dose assuming a standard volume ( $\text{KAD}_{\text{StdVol}}$ ) ranged between 25.6 and 38.6 Gy (Table 2). There was no difference between males and females, and no correlation with age or kidney volume was observed.

Kidney dose computation using MIRD Pamphlet 19 and CT-measured kidney cortex volumes ( $\text{KAD}_{\text{CTVol}}$ ), instead of MIRDOSE3.1 and standard volumes, resulted in a wider range of dose estimates (19.4–39.6 Gy) (Table 2).

Finally, taking into account the biologic effect of dose fractionation, the mean BED, obtained from  $\text{KAD}_{\text{CTVol}}$ , was  $40.4 \pm 10.6$  Gy, ranging from 27.7 to 59.2 Gy.

#### Correlation Between Kidney Dose and Renal Function

No relationship was observed between CLR loss per year and  $\text{KAD}_{\text{StdVol}}$  or  $\text{KAD}_{\text{CTVol}}$  (Figs. 3A and 3B). In contrast, BED strongly correlated with CLR loss per year ( $r = 0.93$ ;  $P < 0.0001$ ). As shown in Figure 3C, this relationship was well adjusted to the modified power exponential function (Eq. 4). Indeed, a clear cutoff can be observed between the 5 patients with substantial impairment of kidney function (CLR loss per year  $>20\%$ ) and the other patients. In addition, it is noteworthy that the 5 patients with high BED and pronounced kidney side effects were treated with a relatively small number of therapeutic cycles (Table 1 and Fig. 3C). A similar relationship was obtained between BED and the percentage of CLR change observed at 18 mo after therapy (Fig. 3D).

#### DISCUSSION

The study indicates that kidney absorbed doses estimated by conventional dosimetry do not correlate with the renal toxicity observed in patients treated with  $^{90}\text{Y}$ -DOTATOC. In contrast, a clear dose–effect relationship was found when additional parameters, such as patient-specific kidney volume and rates at which the absorbed doses were delivered, were considered.

Our data provide evidence that 3 major variables influence the actual  $^{90}\text{Y}$ -DOTATOC renal absorbed dose estimates: distribution of the radionuclide, size of the target organ (i.e., the kidney), and the absorbed dose rate.

Spatial and temporal radionuclide distribution is generally assessed by quantitative imaging obtained at different time points after injection. Unfortunately, the therapeutic agent DOTATOC labeled with  $^{90}\text{Y}$ , a pure  $\beta^-$ -particle emitter, is not suitable for quantitative imaging. The substitution of  $^{90}\text{Y}$  with a positron-emitter isotope of yttrium ( $^{86}\text{Y}$ ) provides an appropriate surrogate to predict the in vivo behavior of the therapeutic compound. Kidney uptake and retention of  $^{90}\text{Y}$ -DOTATOC as measured by PET biodistribution study with  $^{86}\text{Y}$ -DOTATOC varied between patients by a factor of 3 and resulted in a wide range of absorbed doses estimated using the MIRDOSE program (1.18–3.60 mGy/MBq). This is in good agreement with our previous report on a larger number of patients, in which we observed a variation in renal absorbed dose ranging between 1.2 and

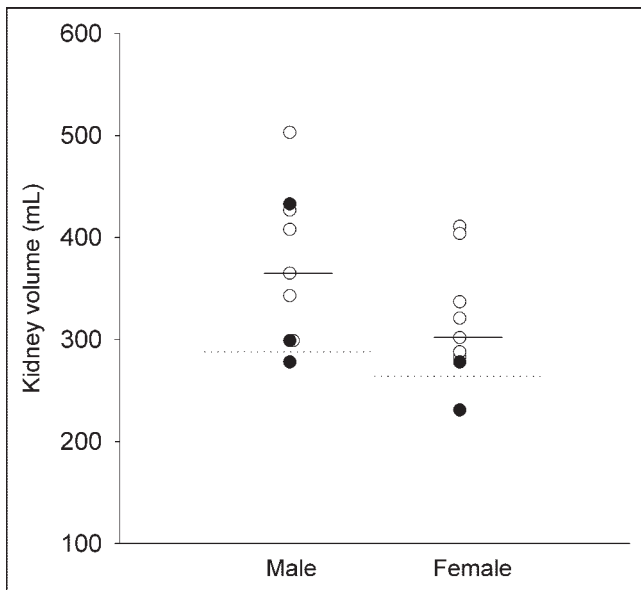


**FIGURE 1.** Individual kidney volumes measured by CT, in males ( $n = 9$ ) and females ( $n = 9$ ). Dotted lines represent standard ORNL phantom values (288 mL in males, 264 mL in females), and continuous lines represent median kidney volumes obtained from CT (365 mL in males, 302 mL in females). Filled circles represent patients with CLR loss per year  $>20\%$ .

5.1 mGy/MBq (10). Such variability of renal radionuclide distribution excludes the possibility of using average individuals and thus underlines the necessity of obtaining individual distribution measurement. Bodei et al. (30), using  $^{111}\text{In}$ -DOTATOC for quantitative imaging and the standard MIRD formalism for dosimetric calculations, also reported wide interindividual differences in renal dose estimates. The use of an  $^{111}\text{In}$ -labeled instead of an  $^{86}\text{Y}$ -labeled surrogate for dose estimation constitutes a promising approach that remains to be validated.

For the estimation of the absorbed dose in the MIRDOSE3.1 software, a standardized phantom value is used for kidney volume (i.e., 288 mL in males and 264 mL in women) (20). The retrospective assessment of individual kidney volumes on pretherapeutic CT showed wide interindividual variability, by as much as a factor of 2. This indicates that individual kidney volume determination is necessary to improve the accuracy of kidney absorbed dose estimation. Recent autoradiography studies performed on human kidney obtained after *in vivo* injection of  $^{111}\text{In}$ -labeled somatostatin analog showed radioactivity to be concentrated in the cortex, mainly in the juxtamedullary region (31). Unfortunately, such precise pattern of activity distribution inside the kidney cannot be determined for each patient by quantitative imaging because of the lack of spatial resolution of PET and SPECT cameras. Therefore, in this study, we considered that the radionuclide accumulated only in the cortical region, which, according to MIRD Pamphlet 19, represents 70% of total kidney volume (24). Although the inclusion of individual renal cortex volumes in

the dosimetry calculations improved dose estimates, no clear dose–effect relationship was observed.

The third variable that was found to be important when implementing absorbed dose estimation was dose fractionation. The rationale of conventional fractionation in external beam radiotherapy is that dividing a dose into several fractions spares normal tissues because of the repair of sublethal damage between dose fractions. The latent period before the onset of radiation-induced functional damage depends on the rate of cell turnover of the tissue. Kidney parenchyma is a slow turnover tissue, and there is a considerable latency before any functional damage is apparent. In external radiotherapy, a dose of 23–27 Gy is considered to result in a 5%–50% probability of developing radiation nephropathy within 5 y after treatment (18). Such a dose is typically administered homogeneously and at a high dose rate in fractions of 1.5–2 Gy. In contrast, the radiation dose delivered during radionuclide therapy with  $^{90}\text{Y}$ -DOTATOC is given at a much lower rate and is exponentially decaying with an effective half-life of approximately 30 h (19). The penetration range of the radiation is shorter, and, as already mentioned, the distribution of the radionuclide within the organs is heterogeneous.

According to the LQ model, it was reported that the critical kidney dose for PRRT was higher than that for external radiotherapy and our results are in agreement (19). The median BED estimated in our patients was 37 Gy. The integration of the dose rate effect in the dosimetry estimation strongly improved the correlation between the resulting

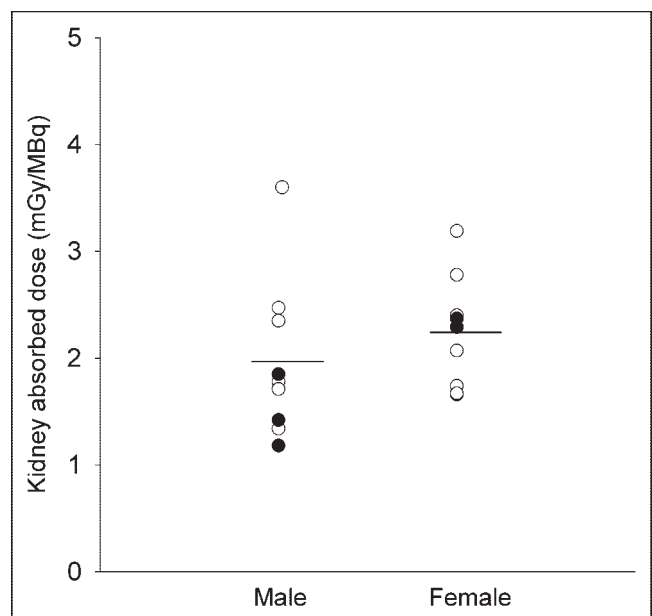


**FIGURE 2.** Individual kidney absorbed dose of  $^{90}\text{Y}$ -DOTATOC, using  $^{86}\text{Y}$ -DOTATOC quantitative imaging. MIRDOSE3.1 was used for dosimetric calculations. Data are reported for males ( $n = 9$ ) and females ( $n = 9$ ). The continuous line represents median kidney dose in each group. Filled circles represent patients with CLR loss per year  $>20\%$ .

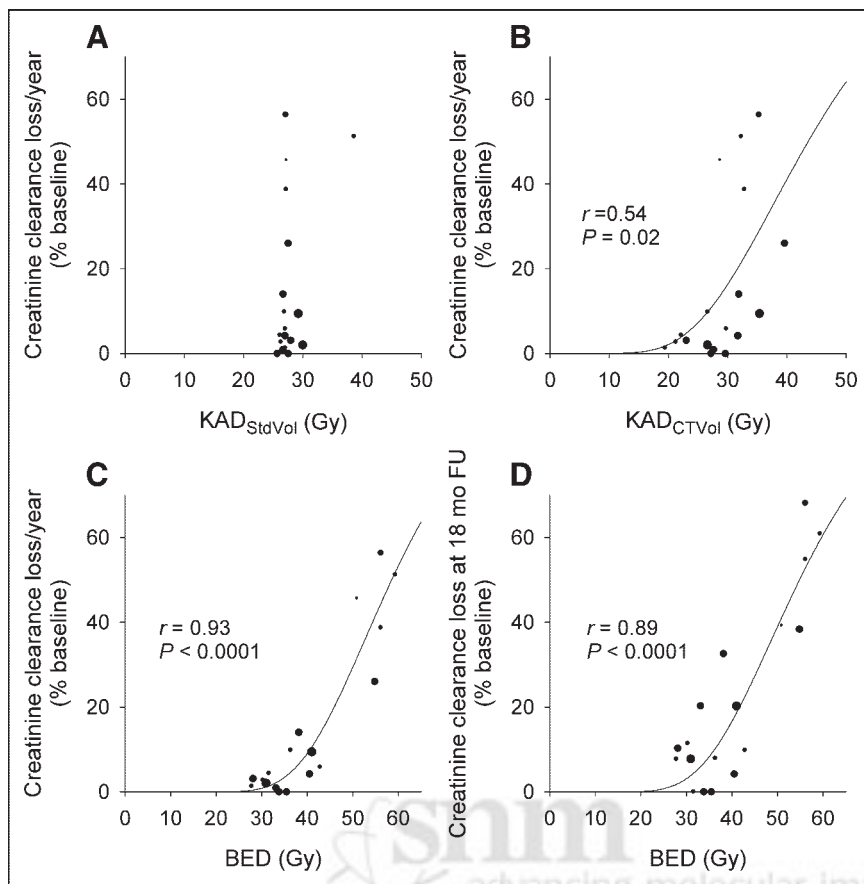


**FIGURE 3.** Correlation between KAD or BED, and the loss in CLR. (A)  $KAD_{StdVol}$  computed by MIRDOSE3.1  $KAD_{StdVol}$ . (B)  $KAD_{CTVol}$  computed by MIRDO Pamphlet 19. (C) Correlation between BED and current CLR loss per year. (D) Correlation between BED and percentage of CLR loss after 18-mo follow-up. Size of symbols reflects number of treatment cycles received by each patient (from 1 for smallest to 5 for largest). Points were fitted to power exponential function (see Eq. 4 in text). In C, note clear difference in BED values observed between patients with rapid CLR decline (CLR loss per year >20%) compared with those with a slower decline.

BED and renal function impairment. It should be noted that the 5 patients with BED values >45 Gy were those who exhibited the most rapid decline in CLR after treatment. Therefore, a BED value of 45 Gy could be proposed as a threshold limit for an increased risk of rapid decline of renal function.

Although our data suggest that the most prominent cause of renal toxicity with PRRT is the absorbed dose to the kidneys, other factors, such as preexisting hypertension, diabetes, or previous chemotherapy, may accelerate renal function loss induced by radiation, possibly by an unsuspected loss of “renal reserve.” It must be kept in mind that in adults the number of nephrons is fixed and would inevitably decrease with time. This means that any damage to functional nephrons is irreparable but may remain clinically and biologically silent, because no simple tests are able to measure the maximum glomerular filtration rate. In this study, only 3 patients had undergone chemotherapy before  $^{90}\text{Y}$ -DOTATOC treatment. Two of them showed only a minor reduction in renal function after treatment. In the third patient, we observed a rapid decline in renal function, but the key role of chemotherapy could not be proven because the patient also had other potential risk factors, such as diabetes and preexisting hypertension. In addition, the latter patient received kidney doses estimated to be twice as high as those received by the 2 other patients. It should be

noted that preexisting hypertension was found in 3 out of the 5 patients with CLR loss per year >20%, suggesting that preexisting hypertension could contribute to the impairment of renal function after therapy. However, a larger number of observations are needed to allow for definite conclusions.

The time appearance and dose-dependence of radiation damage in normal tissue depend on its proliferative behavior. For acutely responding tissues that express damage within a period of days to weeks after irradiation, the  $\alpha/\beta$ -ratio is in the range of 7–20 Gy, whereas for late-responding tissues that express damage months to years after irradiation, that ratio ranges from 0.5 to 6 Gy (32). For the kidney we used the  $\alpha/\beta$ -ratio (2.6 Gy) and half-time of DNA repair (2.8 h) generally accepted in the literature. These values were taken from data in a rodent model (29). Analyses of data from human tissues on DNA repair kinetics are in fact limited. However, the agreement between human and animal data is generally considered acceptable (33). The  $\alpha/\beta$ -value provides a quantitative index of the sensitivity of a given organ or tumor to changes in dose rate. Tissues with low  $\alpha/\beta$ -values, such as kidneys, are more sensitive to small changes in the dose rate or dose per fraction than tissues with high  $\alpha/\beta$ -ratios, such as tumors. According to our results, it should be recommended to fractionate the total administered activities in more cycles to allow the sublethal radiation damage repair in normal tissue.

However, the effect of dose fractionation on tumor response remains to be evaluated. It is generally admitted that the effect on tumors occurs earlier than in the kidney and that the  $\alpha/\beta$ -value is generally higher for tumors (5–25 Gy) than for late-responding kidney (2–3 Gy). The increase in  $\alpha/\beta$ -value for tumors compared with normal tissues has been observed in other cancers (33). Also, the DNA repair half-time is generally shorter in tumor cells (34). With a higher  $\alpha/\beta$ -ratio and a lower DNA repair half-time, the ratio of the quadratic term versus the linear term in Equation 3 decreases, and, as a result, tumors are likely to be less sensitive to fractionation.

## CONCLUSION

The use of a refined absorbed dose methodology led to the finding of a clear kidney dose–response relationship in patients treated with  $^{90}\text{Y}$ -DOTATOC. Our data provide evidence that patient-specific anatomy and dose-rate effects cannot be neglected. The BED model appears to be a reliable predictor of toxicity and could thus be helpful in implementation of individual treatment planning. Considering the complexity of  $^{86}\text{Y}$  quantitative imaging, further studies should evaluate whether dosimetric methods using a widely available tracer such as  $^{111}\text{In}$ -pentetretotide remain accurate enough to predict response.

## ACKNOWLEDGMENT

The authors thank Joëlle De Camps for invaluable assistance in data collection.

## REFERENCES

1. Reubi JC. Peptide receptors as molecular targets for cancer diagnosis and therapy. *Endocr Rev*. 2003;24:389–427.
2. Otte A, Mueller-Brand J, Dellas S, Nitzsche EU, Herrmann R, Maecke HR. Yttrium-90-labelled somatostatin analogue for cancer treatment. *Lancet*. 1998;351:417–418.
3. de Jong M, Valkema R, Jamar F, et al. Somatostatin receptor-targeted radionuclide therapy of tumors: pre-clinical and clinical findings. *Semin Nucl Med*. 2002;32:133–140.
4. Chinol M, Bodei L, Cremonesi M, Paganelli G. Receptor-mediated radiotherapy with  $^{90}\text{Y}$ -DOTA-D-Phe<sup>1</sup>-Tyr<sup>3</sup>-octreotide: the experience of the European Institute of Oncology Group. *Semin Nucl Med*. 2002;32:141–147.
5. Waldherr C, Pless M, Maecke HR, et al. Tumor response and clinical benefit in neuroendocrine tumors after 7.4 GBq  $^{90}\text{Y}$ -DOTATOC. *J Nucl Med*. 2002;43:610–616.
6. Bushnell D, O'Dorisio T, Menda Y, et al. Evaluating the clinical effectiveness of  $^{90}\text{Y}$ -SMT 487 in patients with neuroendocrine tumors. *J Nucl Med*. 2003;44:1556–1560.
7. Kwekkeboom DJ, Mueller-Brand J, Paganelli G, et al. An overview of the results of peptide receptor radionuclide therapy with 3 different radiolabeled somatostatin analogues. *J Nucl Med*. 2005;46(suppl):62S–66S.
8. Pauwels S, Barone R, Walrand S, et al. Practical dosimetry of peptide receptor radionuclide therapy with  $^{90}\text{Y}$ -labeled somatostatin analogues. *J Nucl Med*. 2005;46(suppl):92S–98S.
9. Jonard P, Jamar F, Walrand S, et al. Tumor dosimetry based on PET  $^{86}\text{Y}$ -DOTA-Tyr<sup>3</sup>-octreotide (SMT487) and CT-scan predicts tumor response to  $^{90}\text{Y}$ -SMT487 (Octreother<sup>TM</sup>) therapy [abstract]. *J Nucl Med*. 2000;41(suppl):111P.
10. Jamar F, Barone R, Mathieu I, et al.  $^{86}\text{Y}$ -DOTA<sup>0</sup>-D-Phe<sup>1</sup>-Tyr<sup>3</sup>-octreotide (SMT487): a phase I clinical study—pharmacokinetics, biodistribution and renal

- protective effect of different regimens of amino acid co-infusion. *Eur J Nucl Med Mol Imaging*. 2003;30:510–518.
11. Förster GJ, Engelbach MJ, Brockmann J, et al. Preliminary data on biodistribution and dosimetry for therapy planning of somatostatin receptor positive tumours: comparison of  $^{86}\text{Y}$ -DOTATOC and  $^{111}\text{In}$ -DTPA-octreotide. *Eur J Nucl Med*. 2001;28:1743–1750.
  12. Cremonesi M, Ferrari M, Zoboli S, et al. Biokinetics and dosimetry in patients administered with  $^{111}\text{In}$ -DOTA-Tyr<sup>3</sup>-octreotide: implication for internal radiotherapy with  $^{90}\text{Y}$ -DOTATOC. *Eur J Nucl Med*. 1999;26:877–886.
  13. Otte A, Hermann R, Heppeler A, et al. Yttrium-90 DOTATOC: first clinical results. *Eur J Nucl Med*. 1999;26:1439–1447.
  14. Moll S, Nিকেleit V, Mueller-Brand J, Brunner FP, Maecke HR, Mihatsch MJ. A new cause of renal thrombotic microangiopathy: yttrium 90-DOTATOC internal radiotherapy. *Am J Kidney Dis*. 2001;37:847–851.
  15. Cybulla M, Weiner SM, Otte A. End stage renal disease after treatment with  $^{90}\text{Y}$ -DOTATOC. *Eur J Nucl Med*. 2001;28:1552–1554.
  16. Boerman OC, Oyen WJG, Corstens FHM. Between the Scylla and Charybdis of peptide radionuclide therapy: hitting the tumor and saving the kidney. *Eur J Nucl Med*. 2001;28:1447–1449.
  17. Stoffel MP, Pollok M, Fries J, Baldamus CA. Radiation nephropathy after radiotherapy in metastatic medullary thyroid carcinoma. *Nephrol Dial Transplant*. 2001;16:1082–1083.
  18. Emami B, Lyman J, Brown A, et al. Tolerance of normal tissue to therapeutic irradiation. *Int J Radiat Oncol Biol Phys*. 1991;21:109–122.
  19. Konijnenberg MW. Is the renal dosimetry for [ $^{90}\text{Y}$ -DOTA<sup>0</sup>,Tyr<sup>3</sup>]octreotide accurate enough to predict thresholds for individual patients? *Cancer Biother Radiopharm*. 2003;18:619–625.
  20. Stabin MG. MIRDOSE: personal computer software for internal dose assessment in nuclear medicine. *J Nucl Med*. 1996;37:538–546.
  21. Valkema R, Kvols L, Jamar F, et al. Phase I study of therapy with  $^{90}\text{Y}$ -SMT487 (Octreother<sup>®</sup>) in patients with somatostatin receptor (SS-R) positive tumors [abstract]. *J Nucl Med*. 2002;43(suppl):P120.
  22. Cockcroft DW, Gault MH. Prediction of creatinine clearance from serum creatinine. *Nephron*. 1976;16:31–41.
  23. Valkema R, Pauwels S, Kvols LK, et al. Long-term follow-up of renal function after peptide receptor radiation therapy (PRRT) with [ $^{90}\text{Y}$ -DOTA<sup>0</sup>,Tyr<sup>3</sup>] octreotide and [ $^{177}\text{Lu}$ -DOTA<sup>0</sup>,Tyr<sup>3</sup>]octreotate. *J Nucl Med*. 2005;46(suppl):83S–91S.
  24. Bouchet LG, Bolch WE, Blanco HP, et al. MIRD pamphlet no. 19: absorbed fractions and radionuclide S values for six age-dependent multiregion models of the kidney. *J Nucl Med*. 2003;44:1113–1147.
  25. Rösch F, Qaim SM, Stöcklin G. Production of the positron emitting radioisotope  $^{86}\text{Y}$  for nuclear medical applications. *Int J Appl Radiat Isot*. 1993;44:677–681.
  26. Wienhard K, Dahlböm M, Eriksson L, et al. The ECAT EXACT HR: performance of a new high resolution positron scanner. *J Comput Assist Tomogr*. 1994;18:110–118.
  27. Hudson HM, Larkin RS. Accelerated image reconstruction using ordered subsets of projection data. *IEEE Trans Med Imaging*. 1994;13:601–609.
  28. Walrand SH, Jamar F, Mathieu I, et al. Quantification in PET using isotopes emitting prompt single gammas: application to  $^{86}\text{Y}$ . *Eur J Nucl Med*. 2003;30:354–361.
  29. Thames HD, Ang KK, Stewart FA, van Der Schuren E. Does incomplete repair explain the apparent failure of the basic LQ model to predict spinal cord and kidney responses to low doses per fraction? *Int J Radiat Biol*. 1988;54:13–19.
  30. Bodei L, Cremonesi M, Zoboli S, et al. Receptor-mediated radionuclide therapy with  $^{90}\text{Y}$ -DOTATOC in association with amino acid infusion: a phase I study. *Eur J Nucl Med*. 2003;30:207–216.
  31. de Jong M, Valkema R, van Gameren A, et al. Inhomogeneous localization of radioactivity in the human kidney after injection of [ $^{111}\text{In}$ -DTPA]octreotide. *J Nucl Med*. 2004;45:1168–1171.
  32. Dale R. Use of the linear-quadratic radiobiological model for quantifying kidney response in targeted radiotherapy. *Cancer Biother Radiopharm*. 2004;19:363–369.
  33. Thames HD, Bentzen SM, Turesson I, Overgaard M, Van den Bogaert W. Time-dose factors in radiotherapy: a review of human data. *Radiother Oncol*. 1990;19:219–235.
  34. Joiner MC, van der Kogel AJ. The linear-quadratic approach to fractionation and calculation of isoeffect relationships. In: Steel GG, ed. *Basic Clinical Radiobiology*. London, UK: Arnold; 1997:106–122.